Journal of Power Sources 195 (2010) 2057–2063

Contents lists available at ScienceDirect

Journal of Power Sources

journal homepage: www.elsevier.com/locate/jpowsour

Investigation of the gas-diffusion-electrode used as lithium/air cathode in non-aqueous electrolyte and the importance of carbon material porosity

Chris Tran[a], Xiao-Qing Yang[b], Deyang Qu[a,*]

[a] Department of Chemistry, University of Massachusetts Boston, 100 Morrissey Blvd., Boston, MA 02125, United States
[b] Chemistry Department, Brookhaven National Laboratory, Upton, NY 11973, United States

ARTICLE INFO

Article history:
Received 2 September 2009
Received in revised form 6 October 2009
Accepted 6 October 2009
Available online 13 October 2009

Keywords:
Li–air
Gas-diffusion-electrode
Non-aqueous electrolyte
Porosity
Electrode passivation

ABSTRACT

The gas-diffusion-electrode used in a Li–air cell has been studied in a unique homemade electrochemical cell. Three major obstacles for the development of a feasible Li–air system were discussed with a focus on the development of a functional gas-diffusion-electrode in non-aqueous electrolytes and the way of avoiding the passivation of gas-diffusion-electrodes caused by the deposition of the reduction products. It is the first time that the importance of establishing the 3-phase electrochemical interface in non-aqueous electrolyte is demonstrated by creating air-diffusion paths and an air saturated portion for an air cathode. A model mechanism of electrode passivation by the reaction products was also proposed. Lithium oxides formed during O_2 reduction tend to block small pores, preventing them from further utilization in the electrochemical reaction. On the other hand, lithium oxides would accumulate inside the large pores during the reduction until the density of oxides becomes high enough to choke-off the mass transfer. Carbon materials with a high surface area associated with larger pores should be selected to make the gas-diffusion-electrode for Li–air battery. For the first time, a near linear relationship between the capacity of GDE in a non-aqueous electrolyte and the average pore diameter was demonstrated, which could be used to estimate the capacity of the GDE quantitatively.

1. Introduction

The increased concern about global warming and other environmental issues caused by automobiles has intensified the research and development of electric, hybrid electric, and plug-in hybrid electric vehicles (EV, HEV, and PHEV) internationally. Batteries are the key element for all kinds of EVs, HEVs, and PHEVs. Plug-in hybrid vehicles (PHEVs) are believed to be the next generation of urban commuters. The nature of PHEVs puts a much higher requirement on the energy density of the battery systems. So far, Li-ion is considered the most promising system for PHEVs. The challenge of searching for a battery system with an energy density beyond Li-ion promotes the acceleration of research of metal–air systems. The concept of Li–air chemistry was first introduced by Littauer and Tsai at Lockheed [1]. The use of metallic Li with an air cathode in an organic electrolyte could potentially make a Li–air cell with a capacity 5–10 times higher than the state-of-art Li-ion cells used now [2], giving it the highest theoretical specific energy among any practical redox couples. The average theoretical energy density for the Li–air battery is 8170 Wh kg^{-1}. Although the energy density of the Li–air battery is lower than the energy density of gasoline/air which is 11,860 Wh kg^{-1} [3], the operation efficiency of the former is not limited by the maximum efficiency of the heat engine.

There are two different types of Li–air cells reported in the literature: one is in aqueous and non-aqueous electrolyte [4–6], and another is in uniform non-aqueous electrolyte, which was first reported by Abraham and Jiang [7]. Both systems have attracted a lot of attentions [8–11], especially the impacts of using non-aqueous electrolytes such as organic electrolytes and ionic liquids on the cathode performance, which were investigated in depth recently [12,13]. The overall cell reactions taking place simultaneously during the discharge were believed to be $2Li(s) + O_2(g) \rightarrow Li_2O_2(s)$ and $4Li(s) + O_2(g) \rightarrow 2Li_2O(s)$. The ratio of the two reactions may be determined by the partial pressure of O_2, O_2 concentration, and electrolyte composition [7,8]. It is quite important to note that the work recently published by Bruce [2], in which the electrochemical charging and discharging of Li_2O_2 with the presence of a MnO_2 catalyst were reported. The work reveals a new and important avenue for the research of rechargeable Li–air cells using non-aqueous electrolytes. Recently, Bruce and co-workers screened several other catalysts including α-MnO_2, Fe oxides, Cu oxides, Co oxides and mixed metal perovskite $La_{0.8}Sr_{0.2}MnO_3$ [14–16]. The reduction of the Li oxide was studied in more detail. It was observed that by restricting the depth of discharge, it is possible to obtain good capacity retention on cycling

* Corresponding author. Tel.: +1 617 287 6035; fax: +1 617 287 6185.
E-mail address: deyang.qu@umb.edu (D. Qu).

0378-7753/$ – see front matter © 2009 Elsevier B.V. All rights reserved.
doi:10.1016/j.jpowsour.2009.10.012

and the cyclability may not be limited by the catalyst but more likely by the porosity of the electrode [15].

However, there are still several major obstacles that need to be overcome before the commercialization of Li–air batteries becomes feasible. Along with the efficiency of catalyst, the following three issues are the significant barriers:

1. Development of a functional 3-dimentional 3-phase gas-diffusion-electrode (GDE) in non-aqueous electrolytes.
2. Avoidance of the GDE passivation caused by the deposition of reduction products.
3. Increase of O_2 solubility and diffusion rate in non-aqueous electrolytes.

Oxygen reduction in a non-aqueous electrolyte is substantially different than that in an aqueous electrolyte, such as Zn–air batteries or fuel cells. The O_2 reduction mechanism in non-aqueous electrolytes is primarily through the formation of insoluble Li_2O_2 and Li_2O. Neither O_2^{2-} nor O^{2-} is soluble in a non-aqueous electrolyte, thus the Li_2O_2 and Li_2O will deposit at the location where the charge transfer occurs and O_2^{2-} and O^{2-} form. Unfortunately, this reaction occurs inside the porous electrode, and the solid particles gradually cover the surface, sealing-off pores and eventually inactivating the GDE. In contrast, in the aqueous electrolyte, the products of O_2 reduction are either H_2O_2 or H_2O with no insoluble products at all. Therefore, the GDE can operate for a long time theoretically. Thus, the capacity of a GDE in a non-aqueous electrolyte is limited by the surface available for the deposition and the pore volume available for the storage of the solid reduction products. If Li_2O_2 and Li_2O could not be removed from the matrix of the porous electrode to maintain the active surface of the GDE, the advantage of high capacity for a Li–air battery would be significantly compromised.

The rate of O_2 reduction also relates to the O_2 solubility and diffusion in the electrolyte solution. The O_2 solubility in non-aqueous electrolytes is significantly lower than that in aqueous electrolytes. Therefore, the discharge rate of a Li–air cell would be several orders of magnitude lower than that of a Zn–air or fuel cell, in which the rate for O_2 reduction on a GDE can reach as high as 100 mA cm^{-2} [17], while only 0.5 mA cm^{-2} for Li–air cells was reported in the literature [7,8,12]. Without the substantial increase of both O_2 solubility and diffusion rate in non-aqueous electrolytes, Li–air can only be used in low-rate applications.

In this paper, the results of our studies in the first two issues, the development of a functional 3-dimentional 3-phase GDE in non-aqueous electrolytes, and the avoidance of the GDE passivation caused by the deposition of reduction products are reported. Searching for non-aqueous electrolytes with higher O_2 solubility is making progress in our group and the results will be reported in our future publications.

2. Experimental details

2.1. Materials and gas-diffusion-electrode

High surface area activated carbon materials were purchased from carbon manufacturers. The commercial carbon materials which were selected based on their pore-size distribution profiles, were used as precursors. The as-received carbon materials were reflux washed with acetone in a Soxhlet extractor for 48 h to remove most of the weekly bonded surface functional groups inherited from their raw materials and the manufacturing processes. The carbon materials were then dried and further thermo-treated in a high temperature furnace under a stream and of CO_2 at 800–1000 °C.

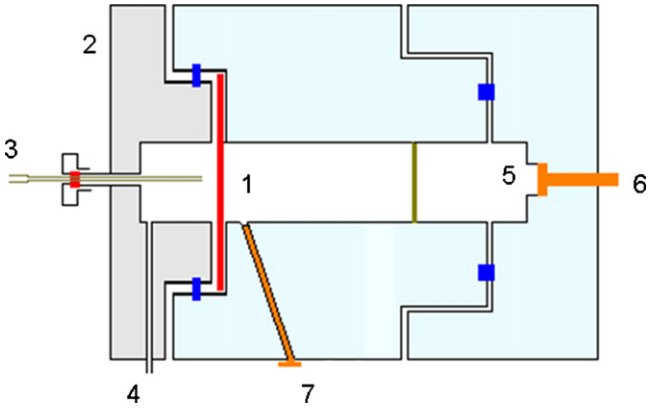

Fig. 1. Electrochemical cell used in the experiments. (1) GDE; (2) cathode top assembly; (3 and 4) air ports; (5) Li counter electrode; (6) anode current collector and (7) reference electrode.

1 M $LiPF_6$ + PC solution was used as the non-aqueous electrolyte. Both battery grade chemicals were purchased from Ferro Corporation and used as received without additional treatments. Metallic Li foil was used as the reference electrode. Unless stated otherwise, all potentials are reported against the Li reference electrode. A Li disk was used as the counter electrode.

A GDE was made with 90 wt% of high surface area carbon and 10 wt% of dry Teflon material. A Teflon suspension (T-30) from DuPont was used. The carbon was first thoroughly mixed with T-30, and the paste was left to air dry. The resulting Teflon-bonded carbon was hot rolled into a thin film and then hot-pressed onto a Ni-mesh current collector using a heavy-duty roller press. The thickness of the finished GDE was 0.008 in. and the weight of the carbon material was 10 mg. All the discharges were done at 1 mA cm^{-2} constant current. No catalyst was used.

Conventionally, mA cm^{-2} is used to present the capacity of a GDE (in either fuel cells or Zn–air cells), because the electrochemical reaction takes place at the 3-phase interface, and theoretically the amount of carbon material should not affect the electrode capacity; mA g^{-1} is normally used to present the capacity of a battery electrode material because the whole electrode will participate in the reaction, and the capacity is determined by the amount of active material. However, GDEs in non-aqueous electrolytes are special. The electrochemical reaction occurs at the 3-phase interface, but the non-soluble reaction products would be stored in the pores of the carbon material. Thus, both the interfacial area and the amount of carbon would have impact on the electrode capacity; however, there seems to be no linear relationship between the capacity and interfacial area or the weight of carbon. As demonstrated by Beattie et al. [9], there was a steep drop-off in specific capacity represented by mA g^{-1}, a sharp increase of specific capacity represented by mA cm^{-2}, as carbon loading is increased. In this paper, the discharge capacity was presented as actual discharge time. For the sake of comparison with the results published in the literature, mA g^{-1} was also included in Fig. 8.

2.2. Electrochemical cell

A Li–air lab cell was made for the investigation. Fig. 1 shows the design of the cell. The carbon side of the GDE (1) is forced against a flat surface by the Ni cathode top assembly (2), which also served as the cathode current collector. The Ni-mesh side of the electrode is against the metal top assembly. An O-ring was placed between the top assembly and cell body to prevent leakage. The interface area is 1 cm^2. On the cathode top assembly, there are two gas ports (3 and 4). O_2 or air can be pumped through the two ports. A metallic lithium disk, as the anode is forced in the cavity (5) against a Ni rod

(6) which is served as the counter electrode. The metallic lithium disk is also served as the reference electrode (7).

2.3. Instrumentation

An EG&G 273 potentiostat/galvanostat controlled by Corrware was used for electrochemical measurements. A Micromeritics ASAP2020 porosimeter was used for the surface area and porosity measurements. Nitrogen was used as an absorbent gas. Density function theory (DFT) software supplied by Micromeritics was used for porosity calculations.

3. Results and discussion

3.1. Porosity of porous carbon material

The total surface area of a powder material is the sum of the surface areas of pores of all sizes. For a given mass, the surface area of the material is inversely related to the size of pores. Thus the surface area of a material that has a high percentage of small pores is larger than that of a material with a high percentage of large pores. Practically, the particles of a fine powder, primary particles, will stick together because of surface forces or binding mechanisms, e.g. Teflon binder and formation pressure, to form secondary particles. Besides the pores in the primary particles, pores are also formed in those aggregated particles. Thus, there are two kinds of pores depending on the formation process; the interstitial pores are formed between the primary particles inside the aggregated particles, and the internal pores are formed within the primary particles. Therefore, the surface area of a solid can be conveniently distinguished between the external and internal surface. External surfaces include all the outer surfaces of particles and aggregated particles, and all the cracks with width-to-depth ratio greater than 1. The internal surface will then be composed of the walls of all cracks, pores, and cavities that are deeper than they are wide.

High surface area carbon materials, especially activated carbon materials, are made by carbonization of hydrocarbon raw materials followed by either thermal or chemical activation to create the pores. The carbon materials are made of hexagonal carbon ring formed atomic layers, which are called “graphene sheets”. These graphene sheets stack together forming primary particles of high surface area carbon; the aggregation of such primary particles forms secondary particles, and pores are formed within and between these aggregated particles. Since the size, orientation, and stacking of these sheets are determined not only by the precursor hydrocarbon material but also by the carbon preparation methods, various carbons have different pore distributions.

The surface area and porosity of a carbon material can be measured experimentally by means of a few techniques depending on the size and type of pores. For example, small-angle X-ray diffraction can be used for the small and close-pores, and mercury intrusion method can be used for large pores. Among all techniques, gas adsorption isotherm (e.g. N_2 adsorption isotherm) is still the most commonly used tool for this purpose. For the high surface area carbon materials, the contributions of micro-pores and meso-pores are dominant. Nitrogen adsorption mechanisms in meso-pores and micro-pores are fundamentally different. The N_2 adsorption onto the surfaces of meso-pores can be correctly described by the classical capillary effect, whereas N_2 adsorption onto micro-pores has to be described by the volume filling mechanism. The major difference between these two processes is the cooperative behavior of the filling gas in the micro-pore, where the influence of the solid surface is still present and the potential fields from neighboring walls overlap. Therefore, the interaction energy of the solid surface with a gas molecule would be correspondingly enhanced in micro-pores, and the density of adsorbed N_2 is higher than in meso-pores [18–20]. Due to the complexity of the adsorption in micro-pores, density function theory (DFT), which relates to a molecular-based statistical thermodynamic theory, is much more suitable than the phenomenological Brunnauer–Emmett–Teller (BET) equation, which would substantially inflates the surface area if applied to a micro-porous material. By means of DFT and with the aid of a fast computer, the whole adsorption isotherm can be fitted, and the pore-size distribution and incremental surface area of pores with various sizes can be calculated. Fig. 2 shows the comparison of the pore-size distribution profiles for two carbon materials prepared in our lab and named as UMB7 and UMB8. The distribution of the surface within the pores of various sizes is clearly illustrated. The smaller pores of the UMB7 carbon material appear to contribute a higher percentage of the surface area than that of UMB8. The “cross-over” point seems to be around 13.5 Å. UMB7 has a larger surface area in the pores with diameter less than about 13.5 Å, while UMB8 starts to show higher surface area when the pore diameters become larger than the “cross-over” 13.5 Å. Table 1 tabulates the adsorption data for the carbon materials used in this study.

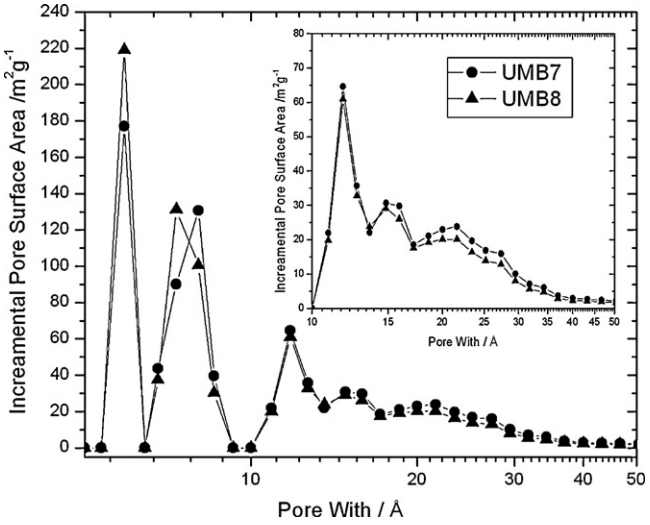

Fig. 2. Comparison of pore-size distribution of activated carbon UMB7 and UMB8 calculated using DFT method from N_2 adsorption isotherm. Inset: enlarged pore-size distribution between 10 Å and 50 Å.

3.2. Electrochemical interface and GDE in non-aqueous electrolytes

The GDE in non-aqueous electrolytes is fundamentally different to that in aqueous electrolytes. Successful development of such GDE is critical to Li–air system. Through the results reported in this paper, it is the first time the significance of such difference is discussed in detail and a potential solution was explored. An efficient porous electrode should not only have a large electrochemically accessible surface area, but also have a large diffusion path for the mass transfer. The electrochemical interfacial reaction, which involves a gas reaction, only takes place when electrolyte and gas molecules co-exist at the same solid electrode interface. The solubility of gas, e.g. O_2 or H_2, in a liquid electrolyte is normally very low. So, the kinetics of the redox reaction of a gas at a completely immersed electrode is limited by the mass transfer rate of gas molecules in the electrolyte. Thus, the current density for a completely immersed electrode is very low, unless a rotation-disk is used. In order to make a highly efficient gas electrode, a sufficient amount of reaction gas has to reach the thin electrolyte film dispersed on the surface of the porous electrode, which connects to the bulk electrolyte. Such an electrode is called

Table 1
Comparison of surface area of carbon, surface area of pore >5 Å, >10 Å, and >20 Å, and average pore diameter.

Sample	Surface of pore >5 Å	Surface of pore >10 Å	Surface of pore >20 Å	Average pore diameter (Å)	Capacity (min)
M20	1450	573	7.7	22.9	14
UMB6	718	221	20.1	36.9	80
UMB7	941	421	47.3	32.1	55
UMB8	904	385	48.8	29.8	34
UMB9	783	213	71.5	54.6	182
UMB10	1211	559	24.0	33.2	56

a "gas-diffusion-electrode" (GDE), as shown in Fig. 3. For a GDE, the side of the electrode facing the electrolyte should be completely wetted by the electrolyte, i.e. all the pores should be filled with electrolyte; the side facing the gas source, however, cannot be occupied by the liquid electrolyte because it has to provide enough of a gas-diffusion tunnels for the gas molecules to migrate to the liquid–solid interface. A GDE is always made with highly porous materials. The electrolyte tends to fill up the pores due to capillary action, and the surface tension will make the liquid electrolyte disperse on the surface of carbon particles and cover a large surface area of the solid electrode with a thin electrolyte film. Within the 3-demensional 3-phase interfacial area, the diffusion channels for both gas and electrolyte interwove with each other and created a large 3-dimensional 3-phase interfacial area. The efficiency of the GDE largely relates to the size of the interfacial area; the larger the area, the more efficient the GDE would be.

In aqueous electrolytes, for example, air cathode for Zn–air cells in alkaline electrolyte and a fuel cell cathode in acidic electrolyte, such a 3-phase interface can be established for a GDE by making the portion facing the electrolyte hydrophilic and the part facing the gas hydrophobic. Then the reaction interface will be at the joint of the hydrophilic and hydrophobic layers. Unfortunately, the surface tension between carbon and most of the non-aqueous electrolytes makes the surface of the carbon easily wetted with organic electrolytes. The portion of the electrode which should be non-electrolyte-flooded gas phase on the air side could also be occupied by the non-aqueous electrolyte. Thus the passage of O_2 in the gas phase to the reaction interface is halted. When a porous electrode is completely wetted by a non-aqueous electrolyte, the pores are all full of the electrolyte, and there is no pathway remaining for gas transfer. After exhausting the small amount of soluble O_2 in the electrolyte, only the double-layer remains to be discharged. Discharge curve 1 in Fig. 4 illustrates this phenomenon. Except for a short period of time for the reduction of dissolved O_2, the rest parts of the discharge curve is more like that of the discharge of a supercapacitor, since a high surface area carbon material was used to make the GDE. However, the GDE started to function normally like a battery cathode when the pressure of O_2 increased slightly above 14 psi or 1 atm. Curves 2 and 3 show the discharge profiles for the GDEs discharged with O_2 pressure at 17 psi and 21 psi, respectively. The hypothesis for the phenomenon is when the O_2 pressure was higher than 1 atm, the electrolyte was forced back from the interface, and the complete wetting of the GDE was avoided. A 3-dimensional 3-phase reaction interface would be created as shown in Fig. 3. Thus, the reduction of O_2 took place at the GDE. Since higher O_2 pressure could create a larger interfacial area to accommodate more reduction products, the same GDE discharged at a higher O_2 pressure demonstrated a higher capacity than that at a lower O_2 pressure. However, too much electrolyte could be pushed out of the porous matrix of GDE if too high gas pressure is applied, reducing the mass transfer in the electrolyte. There are three potential ways to create a 3-dimensional 3-phase reaction interface: slight differential pressure, GDE with starved electrolyte and surface coating which prevents wetting by organic solvents. Read et al. [12] and Yang and co-workers [21,22] reported the effects of high O_2 partial pressure in their studies using the starved non-flooded coin cell design. They attributed the higher discharge capacity obtained by the higher O_2 partial pressure to the increased solubility of O_2 in the non-aqueous electrolyte, and the prevention of the formation of Li_2O_2 film on the carbon surface. It should be pointed out that in both Refs. [12,8], the O_2 partial pressures were as high as 10–11 atm (147–162 psi), while the O_2 partial pressures in this work are in the range of 14–21 psi only. Under such low pressures, neither the solubility of O_2 in the electrolyte nor the formation of Li_2O_2 on the carbon surface could change significantly,

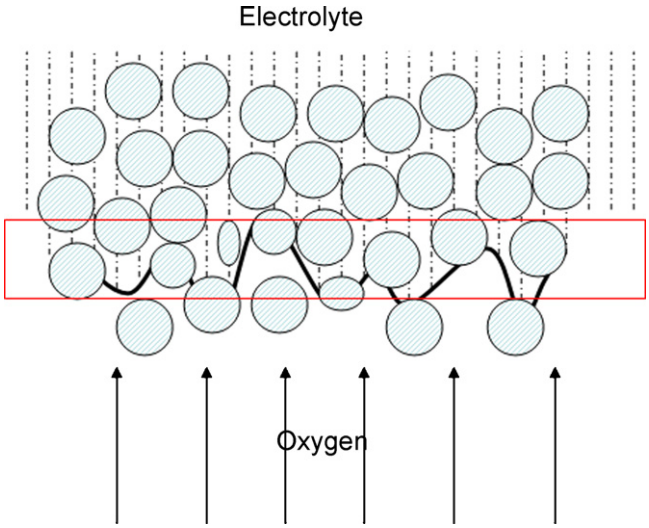

Fig. 3. Schematic of gas-diffusion-electrode.

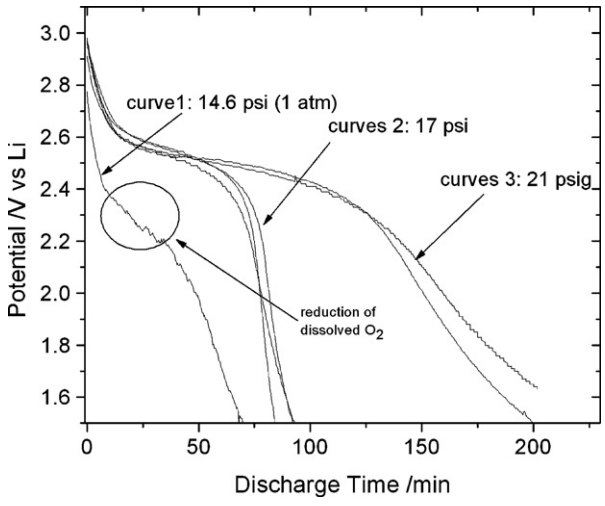

Fig. 4. O_2 reduction on the GDE in 1 M $LiPO_6$ + PC electrolyte at different O_2 pressures. Current density: 1 mA cm^{-2}.

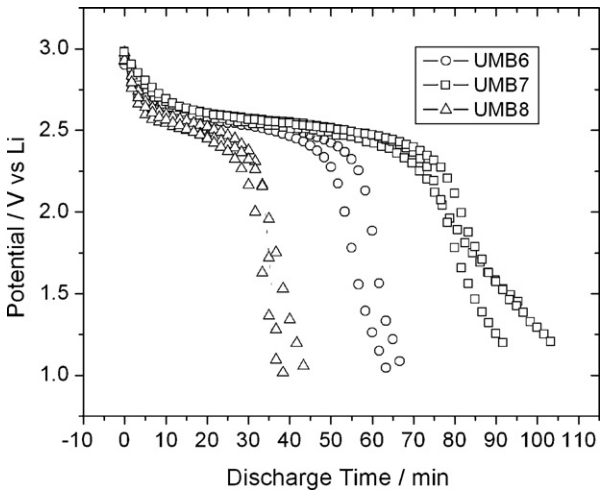

Fig. 5. Comparison of O_2 reduction capacity on the GDEs made with UMB6, UMB7 and UMB8, respectively.

since the O_2 pressure was only slightly above the ambient pressure. It is also worthwhile to point out that in Refs. [12,8], coin cells in a pressurized chamber were used for their studies, where the pressure was uniformly increased. In contrast, only gas pressure through the gas inlet was increased in our investigation. This is much more close to the realistic operation conditions of the Li–air cell, since the cell would leak if a net gas pressure above 10 atm was imposed on GDE without the balancing external high pressure through the pressurized chamber.

3.3. GDE passivation and the selection of carbon materials

The products of O_2 reduction in non-aqueous electrolytes include insoluble Li_2O and Li_2O_2. The GDE ceases to function when the electrode interface is blocked by the Li oxide precipitates. The discharge capacity of a GDE in a non-aqueous electrolyte is dependant on the amount of Li oxide precipitates it can take before ceasing to function. These oxide precipitates accumulate in the porous matrix of the electrode during the discharge process and eventually block the gas and electrolyte transfer to the reaction interface at the carbon surface. Therefore, the porosity of the carbon material plays an important role. Fig. 5 shows the comparison of the discharge capacities of the GDEs made from carbon materials with various porosities but prepared through the same electrode fabrication procedures. The GDEs made from different carbon materials clearly demonstrated different discharge capacities. The difference shown in Fig. 5 is quite substantial. The capacity for the GDE made from UMB7 was more than double to that of UMB8. Conventional wisdom tells us that high surface area is desirable for GDEs, but the results in Fig. 6 tell us that the situation is not so simple. Fig. 6A–C shows the relationship between the O_2 reduction capacity and the surface areas of the pores with diameter larger than 5 Å, 10 Å and 20 Å, respectively. The surface area of pores larger than 5 Å can be considered as the total surface of the carbon material, since it is the minimum pore diameter that can be measured using N_2 adsorption isotherm. There is no simple correlation between the surface areas and the discharge capacity can be drawn, but the discharge capacity is strongly related to the surface area associated with certain size pores. The discharge capacity decreases as the total surface area increases; and the discharge capacity also decreases as the surface area of pores larger than 10 Å increases. However, the trend reversed when the discharge capacity was plotted against the surface area of pores larger than 20 Å. It is quite interesting to point out that the discharge capacity is closely related to the surface area

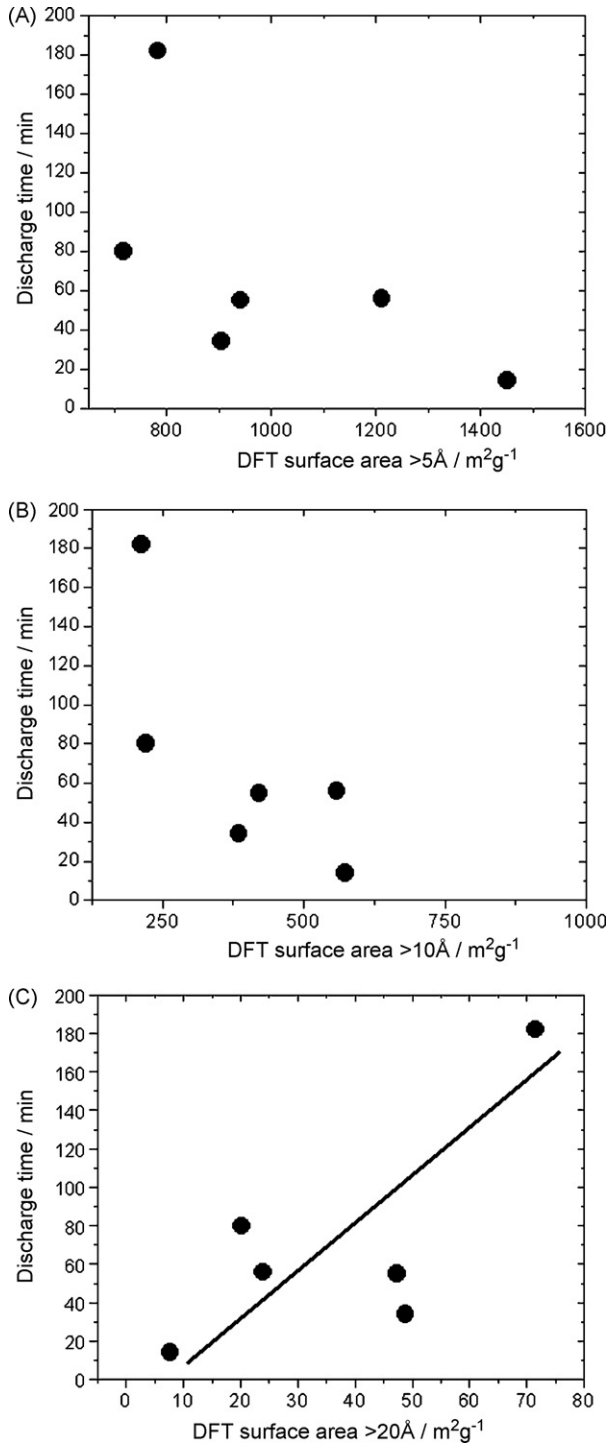

Fig. 6. The relationship between O_2 reduction capacity and DFT surface area of pores with sizes >5 Å (A), >10 Å (B) and >20 Å (C).

associated with pore size larger than 20 Å. The hypothesis for the mechanism of this phenomenon is illustrated in Fig. 7. Since both the O_2^{2-} and O^{2-} formed from the reduction of O_2 are insoluble in a non-aqueous electrolyte, solid Li oxides are likely to be formed near the reaction interface. The interface consists of not only the external surface of carbon particles but also the pore walls inside the porous matrix. The majority of solid Li oxides would be formed inside the micro-, meso-, and macro-pores as shown in Fig. 7. In order for a GDE to function efficiently, both electrolyte and O_2 have to migrate to the reaction interface. In other words, the clear

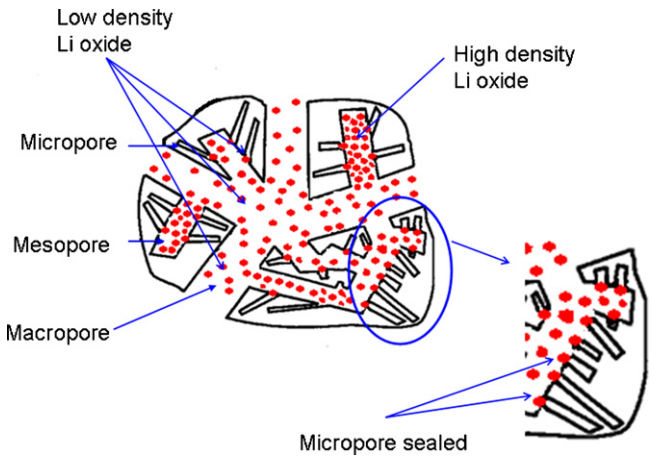

Fig. 7. Accommodation of Li oxides in the pores of various sizes.

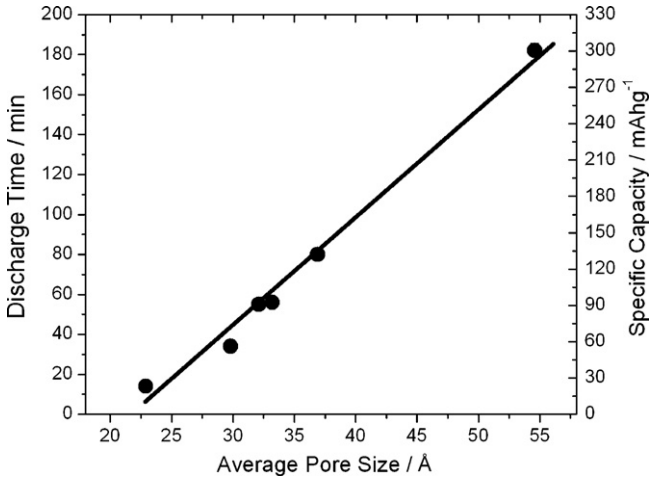

Fig. 8. Discharge time and specific capacity ($mA\,g^{-1}$) as a function of average pore diameter.

pathway for mass transfer has to be maintained. When Li oxide particles are formed near the orifice of a micro-pore as shown in the enlarged inset in Fig. 7, the micro-pore would be sealed and mass transfer in and out of that pore would be blocked because the inside pore surface becomes inaccessible. Since micro-pores comprise most of the surface area for a carbon material with a very high total surface area, rendering them inaccessible substantially decreases O_2 reduction. The experimental results shown in Fig. 6, which demonstrated the discharge capacity for the GDEs made with various high surface area carbon materials, are supportive to this hypothesis. On the other hand, at the early stage of O_2 reduction, the density of the Li oxides formed in the meso-pores and macro-pores was low enough to allow both O_2 and electrolyte diffusion at the interface. Since the particle size of the Li oxides was smaller than the meso- and macro-pore sizes, a substantial amount of precipitates can be accommodated in those pores without hindering mass transfer. However, Li oxides kept accumulating inside the pores as O_2 reduction continued. The density of the Li oxides in the large pores kept increasing and mass transfer through the Li oxides became more and more difficult. Eventually, the pores were blocked and the GDE ceased functioning. The GDE failure mechanism is very similar to that of alkaline fuel cells, in which the pores of GDEs could be blocked by $CaCO_3$, which is the product of carbonation between an alkaline electrolyte and CO_2 in the air. Fig. 8 shows the relationship between average pore diameter and the discharge capacity (measured by the discharge time) for the GDEs. It shows that the discharge capacity increases almost linearly with the increase of average pore diameter. Fig. 8 provides convincing experimental evidence for the hypothesis we proposed. The large pores in the carbon could accommodate much more Li oxide precipitates than small pores. Thus, the utilization for the surface area in the large pores was much higher than that in the small pores. In summary, although larger surface area carbon is in general more desirable for a high rate air cathode, the discharge capacity may suffer, since most of the surface area inside the smaller pores could not be utilized for O_2 reduction when solid Li oxide precipitates on the pore openings and prevents the internal surface from participating in the electrode reaction by blocking mass transfer. On the other hand, Li oxides could reside in the larger pores (for example, those with pore size larger than 20 Å). The GDE ceases to function only when the density of the oxides becomes high enough to block all mass transfer. Thus the capacity of GDEs used in Li–air cells is determined by the surface area of large pores, not the surface area of total pores. Based on the relatively linear relationship, the capacity of a GDE in a non-electrolyte could be estimated quantitatively for the first time through our studies reported here.

It is worthwhile to discuss the capacity of a GDE. Unlike other electrode materials, which themselves participate in the electrochemical reaction, the carbon in the GDE is inert and only provides the sites for the O_2 reduction. Thus, its capacity should not be limited, assuming the physical properties of the GDE are unchanged. The capacity of the GDE in non-aqueous electrolytes is limited by the precipitation of the reduction products. Recharging the GDE would bring it back to life again [2], but the ultimate goal is to prevent the accumulation of Li oxides on the GDE in order to make the Li–air cell appealing for practical applications. Such research is in progress in our lab and the results will be reported in a later publication.

4. Conclusion

The nature of high surface area carbon materials and the relationship between the pore-size distribution and the GDE performance in a Li–air cell have been elucidated by means of traditional electrochemical discharge and porosimetry. The following points are of value to be noted:

(1) A 3-phase interface is essential for a GDE. Gas-diffusion paths and an air saturated portion need to be created. The behavior of double-layer capacitance, rather than a battery behavior would be the dominating electrochemical phenomenon if the electrode is completely soaked with non-aqueous electrolyte. O_2 pressure which is slightly higher than ambient pressure is enough to force the electrolyte back and create the desirable 3-phase interface on the GDE.
(2) Micro-pores and some of meso-pores would be blocked by Li oxides formed at the beginning of discharge through the reduction of O_2, and the surface area of those pores will not be accessed by either air or electrolyte, making them unavailable for the electrochemical reaction.
(3) The majority of the solid Li oxides reside inside the large pores. The density of the oxides increases as the reduction proceeds until the density is high enough to completely block mass transfer. Thus, the capacity of the electrode is determined by the amount of Li oxides that the large pores can accommodate without jeopardizing mass transfer.
(4) The capacity of a GDE in a non-electrolyte was found to have an almost linear relationship with average pore diameter of carbon. Such a linear relationship could be used to estimate the capacity of a GDE in non-aqueous electrolyte quantitatively.

Acknowledgments

The work was supported by the Assistant Secretary for Energy Efficiency and Renewable Energy, Office of Vehicle Technologies, under the program "Hybrid and Electric Systems," of the U.S. Department of Energy under Contract Number DEAC02-98CH10886. The work at UMB was also partially supported through the UMB faculty start-up grant. Both financial supports are gratefully acknowledged.

References

[1] E.L. Littauer, K.C. Tsai, J. Electrochem. Soc. 123 (1976) 771–776.
[2] T. Ogasawara, A. Debart, M. Holzapfel, P. Novak, P.G. Bruce, J. Am. Chem. Soc. 128 (2006) 1390–1393.
[3] S.S. Sandhu, J.P. Fellner, G.W. Brutchen, J. Power Sources 164 (2007) 365–371.
[4] T. Zhang, N. Imanishi, S. Hasegawa, A. Hirano, J. Xie, Y. Takeda, O. Yamanoto, N. Sammes, J. Electrochem. Soc. 155 (2008) A965–A969.
[5] S. Hasegawa, N. Imanishi, T. Xhang, J. Xie, A. Hirano, Y. Takeda, O. Yamanoto, J. Power Sources 189 (2009) 371–377.
[6] T. Zhang, N. Imanishi, S. Hasegawa, A. Hirano, J. Xie, Y. Takeda, O. Yamanoto, N. Sammes, Electrochem. Solid-State Lett. 12 (2009) A132–A135.
[7] K.M. Abraham, Z. Jiang, J. Electrochem. Soc. 143 (1996) 1–12.
[8] J. Read, J. Electrochem. Soc. 149 (2002) A1190–A1195.
[9] S.D. Beattie, D.M. Masolescu, S.L. Blair, J. Electrochem. Soc. 156 (2009) A44–A47.
[10] Z.P. Zheng, R.Y. Liang, M. Hendrickson, E.J. Plichta, J. Electrochem. Soc. 155 (2008) A432–A437.
[11] S.J. Visco, M.Y. Chu, USP 6,025,094.
[12] J. Read, K. Mutolo, M. Ervin, W. Behl, J. Wolfenstine, A. Driedger, D. Foster, J. Electrochem. Soc. 150 (2003) A1351–A1356.
[13] T. Kuboki, T. Okuyama, T. Ohsaki, N. Takami, J. Power Sources 146 (2005) 766–769.
[14] A. Debart, A.J. Paterson, J. Bao, P.G. Bruce, Angew. Chem. Int. Ed. 47 (2008) 4521–4524.
[15] A. Debart, J. Bao, G. Armstrong, P.G. Bruce, J. Power Sources 174 (2007) 1177–1182.
[16] A. Debart, J. Bao, G. Armstrong, P.G. Bruce, ECS Trans. 27 (2007) 225–232.
[17] N. Ominde, N. Bartlett, X.Q. Yang, D.Y. Qu, J. Power Sources 185 (2008) 747–753.
[18] S.J. Gregg, K.S.W. Sing, Adsorption, Surface Area and Porosity, Academic Press, London, 1982.
[19] P.A. Webb, C. Orr, Analytical Methods in Fine Particle Technology, Micromeritics Instruments Corporation, GA, 1997.
[20] J.S. Oliver, J. Porous Mater. 2 (1995) 9–17.
[21] X.H. Yang, Y.Y. Xia, J. Solid State Electrochem 14 (2010) 109–114.
[22] X.H. Yang, He Ping, Y.Y. Xia, Electrochem. Commun. 11 (2009) 1127–1130.